Hardness-load modelling applied to multilayer galvanised coatings

Y. Benarioua[1], A. Mejias[2,3], F. Roudet[2], A. Iost[4] and D. Chicot[2]*

During the last past decades, galvanised steels have been extensively developed to improve corrosion resistance of steels due to their excellent chemical properties particularly in severe atmospheric conditions. The objective of this work is to predict the hardness-load variation in relation to the bath immersion time using both a multilayer coating hardness model and a layers growth modelling. The kinetic growth of each layer relates the thickness to the immersion time by a simple power law. The hardness of the intermetallic compounds is determined by applying a multilayer hardness model on classical Vickers microindentation data obtained at different indentation loads. Afterwards by combining the kinetic growth laws and the compounds hardness, it is possible to predict the surface hardness-load variation as a function of the immersion bath time.

Keywords: Steel, Zinc, Iron, Galvanisation, Hardness, Modelling

Introduction

The use of zinc metallic or zinc–iron alloyed coatings deposited onto steel is one of the most important commercial processing techniques employed to protect steel components exposed to severe corrosive environments. The principle of galvanising has not changed during these 200 last years,[1–8] but the development of recent applications under more severe conditions led to a development of new galvanised processes like hot-dip galvanising.[9–11] Whatever the process employed, a multilayer coating is formed that renders difficult the prediction of the mechanical properties. This has motivated the present work in which we propose a hardness-load modelling to predict the hardness for a given bath immersion time.

Within this objective, it is necessary to study the relationship between the bath immersion time and the coating thickness as well as the determination of the layers hardness. The kinetic growth of each layer is represented by a simple power law connecting the layer thickness to the bath immersion time. Afterwards, the multilayer hardness model developed by Rahmoun *et al.*[12] extended by Puchi-Cabrera *et al.*[13] was applied to determine the hardness of each layer. Finally, from the relation between the layers thickness and the bath immersion time in association with the identification of the hardness of each intermetallic compound, the proposed methodology allows the plot of the hardness-load variation for a given bath immersion time.

[1]Département de Génie Mécanique, Faculté de Technologies, Université de M'Sila, BP 166, M'Sila, 28000, Algérie
[2]Univ. Lille, FRE 3723 - LML - Laboratoire de Mécanique de Lille, F-59000 Lille, France
[3]Facultad de Ingeniería, Laboratorio de Materiales, Universidad de Carabobo, Valencia, Venezuela
[4]Arts et Métiers ParisTech, MSMP, ENSAM 8, Boulevard Louis XIV, F-59046 Lille, France

*Corresponding author, email: didier.chicot@univ-lille1.fr

Experiments

The substrate is a low-carbon steel with the following chemical composition: 0·17%C, 1·40%Mn, 0·045%P and 0·045%S in weight percent. Prior to the galvanisation, the specimens were initially degreased, pickled in an aqueous solution containing 16% of H_2SO_4 and fluxed in an aqueous solution containing $ZnCl_2$ and $2NH_4Cl$. Afterward, the samples were dipped into the galvanising bath containing the chemical composition: 0·20%Cd, 1·4%Pb, 0·05%Fe, 0·01%Cu, 3·5%Al and Zn in balance. During the different immersion times ranging from 1 to 300 min, the coatings were carried out in the galvanising bath at the temperature of 450°C and then quenched immediately in water to preserve the galvanising structure. The structure of the coatings is analysed by X-ray diffraction using a Philips MPD diffractometer with a monochromatic Co (Kα) radiation. The microstructure observations and the thickness measurements were both performed on a Nikon optical microscopy. Hardness was determined using a Leco microhardness tester equipped with a Vickers indenter. Three indentation experiments were performed at each indentation load in order to obtain a representative hardness value. The hardness-depth profile along a cross-section was obtained by applying 0·25 N of indentation load. To apply the multilayer model, normal indentation loads ranging between 0·1 and 200 N have been applied at the surface of the coating.

Iron–zinc phase formation

For classical galvanising temperatures, Horstmann[1,6] suggested that the layers are mainly formed of zinc

saturated α-iron, Γ-phase layer, δ-phase layer, ξ-phase layer and η-phase layer.[2] However, accordingly with the Fe–Zn binary diagram, double layers of gamma (Γ_1-Fe_5Zn_{21} and Γ-Fe_3Zn_{10}) phases can be formed at the interface between iron and δ-phase layer. Between 550 and 665°C, only the gamma (Γ) phase layer is stable along with the constant domain delta (δ-$FeZn_{10}$) phase. Above the temperature of 665°C, the delta (δ) phase layer is no longer stable and only the gamma (Γ) phase is formed. Since there is no evidence for flaking of the gamma (Γ) phase layer, this layer probably grows in the linear region just as it grows in both the lower parabolic and upper parabolic regions.[6] The zeta phase (ξ-$FeZn_{13}$) contains approximately 5–6 wt-% of iron.[2] This phase is formed from the peritectic reaction between the delta (δ) phase and the eta (η) phase which present a liquid of zinc containing iron solute. Although older iron–zinc equilibrium phase diagrams show the existence of both δ_p-$FeZn_7$ phase and δ_k-$FeZn_{10}$ phase, the X-ray diffraction analysis by Bastin *et al*.[8] indicates that only one delta phase exists up to 670°C. The chemical formulation, the crystallographic structure and the hardness of the different phases of zinc–iron compounds which could be encountered in this study are collected in Table 1.

The primary phases formed during the immersion in the galvanising bath are gamma (Γ), delta (δ), zeta (ξ) and eta (η). The Γ phase appears as a layer located close to the base material only when the immersion time is relatively important. The δ and ξ phases are positioned between the two inner and outer layers. The δ phase presents two contiguous layers (δ_k and δ_p) which present the same main physical characteristics but different metallographic structure. The phase δ_k is more compact, whereas the phase δ_p presents a thin continuous strip toward the Γ phase and a thicker strip micro-cracked close to the ξ phase. Adjacent to the delta (δ) phase layer, the zeta (ξ) phase grows in a columnar morphology which is supersaturated in iron. The zeta (ξ) phase has two layers depending upon the super-saturation of iron in the melt. The η phase is the outer phase found in this type of coatings. This phase is mainly composed of pure zinc element and formed at the surface during the solidification of the coating.

Results and discussion

Morphology and microstructure

X-ray diffraction spectra of the galvanised coatings have revealed the presence of the phases η-Zn, ξ-$FeZn_{13}$, δ_k-$FeZn_7$ and δ_p- $FeZn_{10}$. According to the galvanisation conditions employed in this work, no inner phase of Γ is detectible by XRD. Figure 1 shows the typical microstructures of the coating obtained after 15, 60 and 300 min of bath immersion times.

The phase Γ-Fe_3Zn_{10} appears as a black line in a very thin layer with a planar interface between steel and the delta (δ) phase. The δ-phase presents a columnar morphology as a result of a preferred growth perpendicular to the interface. Finally, two distinct zones, the compact δ_p-$FeZn_7$ layer at the neighbourhood of the Γ-Fe_3Zn_{10} layer and the δ_k-$FeZn_{10}$ layer grow nearly of the intermetallic compound ξ-$FeZn_{13}$. Adjacent to the delta (δ_k) phase layer, ξ-$FeZn_{13}$ phase grows in a columnar morphology. Note that the two intermediate and contiguous layers grow before the formation of the subsurface layer of η-Zn phase. The phases formed during a long immersion time in the galvanising bath were eta (η), zeta (ξ), delta (δ_k or/and δ_p) and gamma (Γ or/and Γ_1). Each of these iron–zinc intermetallic phases found in hot-dip galvanised coatings appears following the iron content increasing. In the present work, the solid solution obtained by galvanisation treatment depends on the immersion time. For low bath immersion times, the obtained phase layers were η, ξ and δ_k or/and δ_p, whereas for intermediate and longest periods, the total galvanisation coating presents the following intermetallic compounds: η, ξ, delta (δ_k or/and δ_p) and Γ.

Kinetic growth

The thickness for the different phases present into the galvanising coating and the total thickness of the coating are represented as a function of the bath immersion time in Fig. 2 where Y is the layer thickness expressed in μm and t is the immersion time in min.

As it is expected the total thickness of the galvanisation coating increases when increasing the bath immersion time and reaches 300 μm after 300 min of immersion time. For low immersion times, the phase ξ-$FeZn_{13}$ is predominant in terms of thickness compared to the δ-$FeZn_{10}$ phase which is more significant for the highest immersion times. When the bath immersion time increases, metallographic observations show that after 300 min, the fringe of Γ-phase is formed between the steel substrate and the δ-layer. Variation of layer thickness related to each phase can be explained through the kinetic growth of different solid solutions in galvanisation baths. Horstmann[1,6] reported that there is an overall inward movement of the Γ-phase layer towards the steel, whereas the

Table 1 Chemical formulation, structure and hardness of the different Fe–Zn phases.

Phase	Chemical formulation	Crystallographic structure	Hardness HVN (GPa)	Characteristics	References
α-Fe	Fe(Zn)	BCC	1·04	–	–
Γ	Fe_3Zn_{10}	BCC	3·36	–	2
Γ_1	Fe_5Zn_{21}	FCC	5·05	–	2
δ_k	$FeZn_7$	Hexagonal	2·58–2·80	Very brittle	10
δ_p	$FeZn_{10}$	Hexagonal	2·73–3·58	Very brittle	5
			2·00		10
ξ	$FeZn_{13}$	Monoclinic	1·40	Brittle	2
			1·18–2·08		5
			1·08–1·18		10
η-Zn	(Fe)Zn	HCP	0·52	Ductile	2
			0·41–0·52		5,10

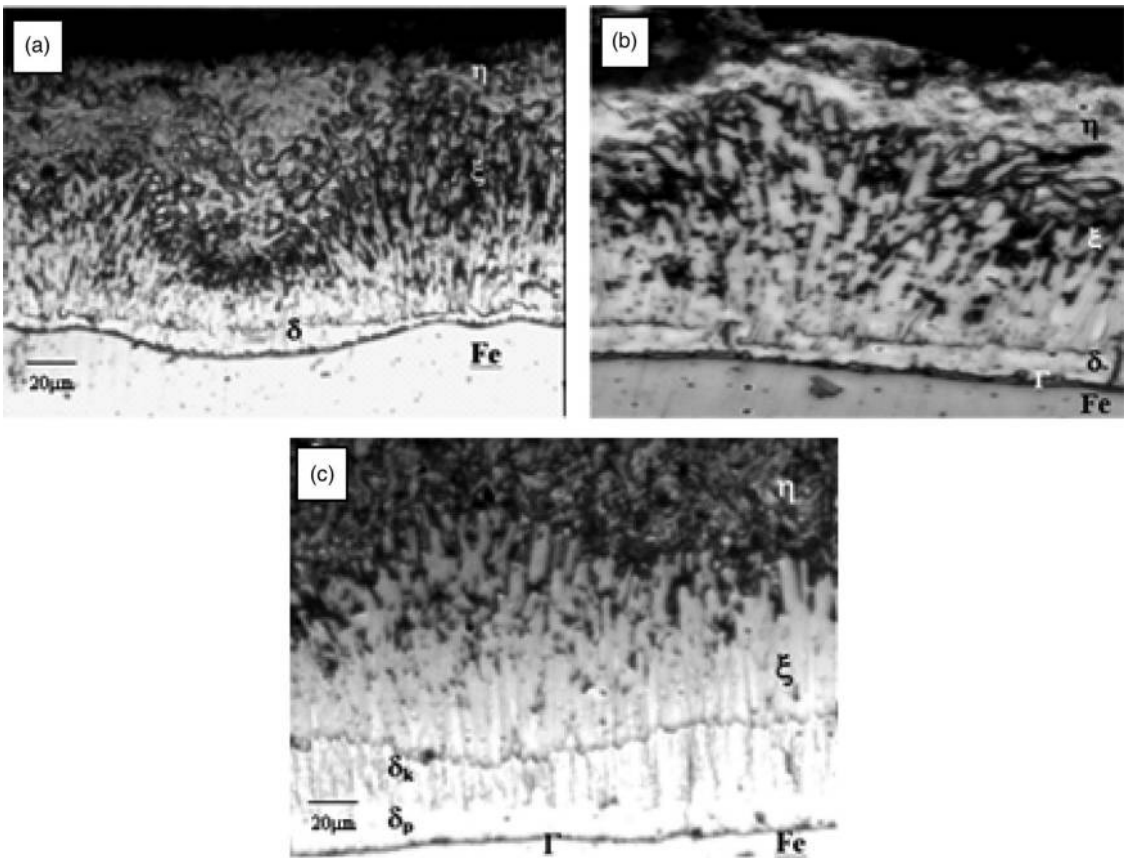

1 Optical micrographs of the coatings obtained at different immersion times: *a* 15, *b* 60 and *c* 300 min.

ξ-phase layer is displaced towards the zinc melt. The δ-phase layer expands in both directions, but generally towards the zinc melt.

To evaluate the kinetic growth of the different intermetallic layers, a simple power-law expressing the growth equation is generally used to interpret the growth rate data,[1] as follows:

$$Y = Kt^n \tag{1}$$

Where Y is the layer thickness expressed in µm and t is the immersion time in min. K and n are fitting parameters representing, respectively, the growth rate constant and the growth rate time exponent.

A better representation of equation (1) is obtained plotting the layer thickness Y as a function of the immersion time t in bi-logarithmic scales in order to highlight a linear representation of the experimental data (Fig. 3). Figure 3 clearly shows that equation (1) represents adequately the experimental data. Table 2 collects the kinetic growth coefficients related to each phase and to the whole coating. The growth rate time constant, n, indicates the type of kinetic governing the growth of layers.

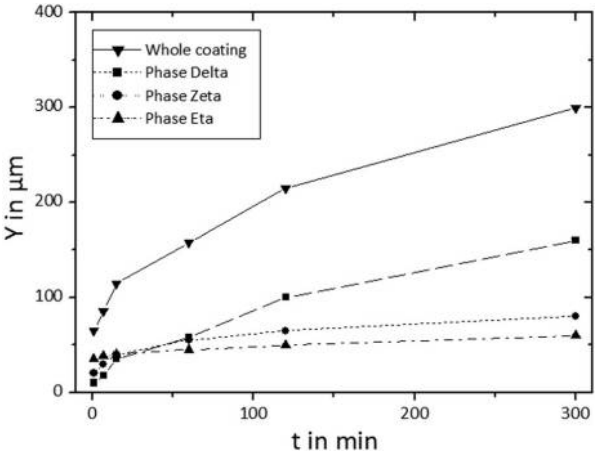

2 Layers and coating thicknesses (Y) as a function of the bath immersion time.

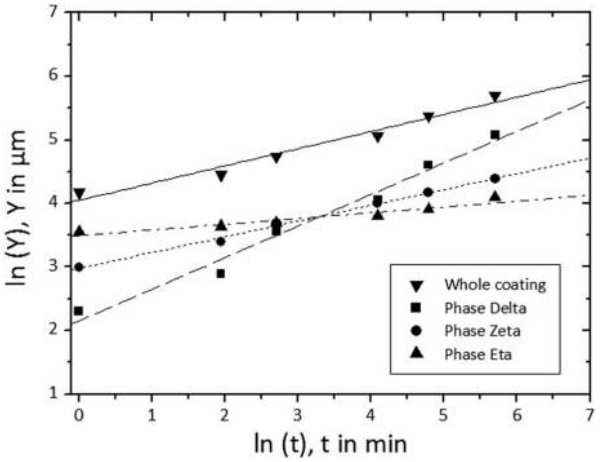

3 Variation of the thickness of each layer and of the whole coating as a function of the bath immersion time in bi-logarithmic scale.

Table 2 Growth rate constant expressed in μm/min^n and growth rate time exponent of the layers and the coating

kinetic growth coefficients	K (μm/min^n)	*n*
δ-$FeZn_7$	8·6	0·50
ξ-$FeZn_{13}$	19·7	0·25
η-Zn	32·8	0·09
Whole coating	57·4	0·27

When the value of n equals 0·5, the growth is controlled by a parabolic diffusion whereas when n equals 1·0, the phase progression is represented by a linear kinetic in which the growth is controlled in the interface.[2] In this work, the values of the growth rate time constant indicated in Table 2 are equal to 0·5 for the δ-phase only, thus confirming that kinetic controlling the growth of the δ-layer is governed by a parabolic diffusion. It notes that values of n both for the ξ-phase and η-phase layers are lower, around 0·25 and 0·09, respectively. Jordon and Marder[5] studying the kinetic growth of different galvanising layers concluded that the growth of the δ-phase layer was parabolic with values of n around 0·5. However, they found lower values for the ξ-phase and the Γ-phase, around 0·35 and 0·25, respectively. In this case, these authors indicate that the kinetics are linear. On the other hand, Horstmann and Peters[4] found that up to 500°C, the total layer kinetic for long immersion times is parabolic. In the present work, the value of n seems to indicate that the kinetic growth is linear since n is equal to 0·25.

Hardness

To study the hardness of multilayer coatings, only the model developed by Rahmoun *et al.*[12] extended by Puchi-Cabrera *et al.*[13] is able to separate the contributions of each layer of the total composite hardness measurement. This model is based on the geometrical model proposed by Jönsson and Hogmark[14] which expresses the composite hardness, H_C, as a function of the film hardness, H_F, and the substrate hardness, H_S, as follows:

$$H_C = a_F H_F + (1 - a_F) H_S \tag{2}$$

Where a_F is the volume fraction of the coating contributing on the composite hardness.

Jönsson and Hogmark[14] proposed that a_F was expressed as a function of the indentation depth, h, the coating thickness, t_F and a constant C linked to the indentation behaviour of coating material and indenter geometry[14]:

$$a_F = 2\frac{C \cdot t_F}{h} - \frac{C^2 \cdot t_F^2}{h^2} = 1 - \left(1 - \frac{C \cdot t_F}{h}\right)^2 \tag{3}$$

The indenter displacement can be directly connected to the indent diagonal d based on simple geometrical considerations of the Vickers indenter tip angles, i.e. $h=d/7$. Additionally for a Vickers indenter, the value of C equals to 0·0728 when the coating fractures, whereas C equals 0·1403 when the coating deforms plastically. Considering that the volume fraction of the coating material must accomplish that: $0 \le a_F \le 1$, equation (3) is ill-defined, since if $C \cdot t_F > h$ then a_F does not reach the unit, as it must do it. Accordingly, Rahmoun *et al.*[12] proposed that a_F is equal to 1 when the product $(C.t_F)$ is higher than the indenter displacement h.

For a multilayer coating formed by N layers, the contribution from volume fraction of the first coating layer to the composite hardness is defined by

$$a_F^{(1)} = \begin{cases} 1 & \text{if } C^{(1)} \cdot t_F^{(1)} > h \\ 1 - \left(1 - \dfrac{C^{(1)} \cdot t_F^{(1)}}{h}\right)^2 & \text{otherwise} \end{cases} \tag{4}$$

And, for the jth layer of the coating

$$a_F^{(j)} = \begin{cases} 1 - \sum_{i=1}^{j-1} a_F^{(i)} & \text{if } \sum_{i=1}^{j} C^{(i)} \cdot t_F^{(i)} > h \\ 1 - \left(1 - \dfrac{\sum_{i=1}^{j} C^{(i)} \cdot t_F^{(i)}}{h}\right)^2 - \left[1 - \left(1 - \dfrac{\sum_{i=1}^{i-1} C^{(i)} \cdot t_F^{(i)}}{h}\right)^2\right] & \\ \text{otherwise} & \end{cases} \tag{5}$$

In equation (5) is observed that the contribution from the volume fraction of jth coating layer to the composite hardness is computed from the difference between the volume fraction of such layer and the previous one. The fraction volume of each layer is calculated on the basis of equation (3), meaning that the volume fraction of the jth layer by means of equation (3) is assessed by subtracting the volume fractions of the priors layers. The volume fraction of the substrate material contributing with the composite hardness can be computed by

$$a_F^{(S)} = 1 - \sum_{i=1}^{N} a_F^{(i)} \tag{6}$$

In this manner, the composite hardness expressed in equation (2) can be rewritten for a multilayer coating system as follows:

$$H_C = a_F^{(S)} \cdot H_S + \sum_{i=1}^{N} \left(a_F^{(i)} \cdot H_F^{(i)}\right) \tag{7}$$

Embracing equation (4) to (7), the composite hardness as a function of the indentation depths for a multilayer coating system can be modelled and computed. The value of the hardness of each coating layer, $H_F^{(i)}$, is estimated by means of a non-linear least square fitting, and from the usually well-known substrate hardness. Furthermore, the variables $a_F^{(i)}$ and $a_F^{(j)}$ are used to represent the contribution of the volume fraction of each layer to the composite hardness, $a_F^{(S)}$ denotes the contribution from the volume fraction of substrate to the composite hardness H_C, and for the ith layer, $C^{(i)}$ denotes a value depending on the indentation behaviour of the material and on the geometry of the indenter, $t_F^{(i)}$ represents its thickness, and $H_F^{(i)}$ is its hardness.

To apply this model, the constants C must be known. $C^{(1)}$ in the equation (4) and $C^{(i)}$ in equation (5) is a parameter only depending on the nature of the film, and it rests as a constant for all film thicknesses. In an indentation test with a Vickers diamond indenter this constant is 0·1403[14] when a hard film is plastically deformed on a soft substrate. This means that the contribution of the substrate to the composite hardness begins at around 14% of the normalised indentation depth instead of the 10%

rule suggested by Bückle[15,16]. If this value is greater, it means that substrate hardness influences hardness measurement for higher indentation depths, as it has been observed in other film/substrate systems[17,18]. Normally, this phenomenon occurs when the film is softer than substrate and thus plastic deformation can occur entirely into the soft film before the indenter tip reach the film/substrate interface.[14] Chen and Vlassak[19] demonstrated that even if the indentation depths reach around 50% of soft film thickness, the composite hardness is not influenced by a harder substrate. C is 0·0728 when indentation test is realised with a Vickers diamond indenter if the coating fractures.[14]

Previous investigation has demonstrated that it exists compression plasticity into the Γ-and ξ-phases, and they have shown that the plastic deformation for the Γ-phase is more than 4% instead of the 0·5% that is reached for the ξ phase.[20] The phases Γ_1 ($Fe_{11}Zn_{40}$), δ_{1k} ($FeZn_7$) and δ_{1P} ($FeZn_{10}$) did not show any plastic deformation before the failure.[21] The fact that the phases, Γ_1, δ_{1k} and δ_{1P} are between the two ductile phases, it may be that during the deformation process, cracks nucleate and grow but the ruptured fragments remain into the coating due to the plastic deformation occurring in the ξ-phase and the Γ-phase which lies in direct contact with the substrate[21]. Note that regarding the fact that the Γ-phase is only observable in a very thin film, associated with the black line at the interface (Fig. 1), this intermetallic compound will be negligible in the following hardness analysis. The hardness measured at the surface of the galvanisation coating under various indentation loads ranging between 0·1 and 200 N is presented in Fig. 4 as a function of the indentation depth for the different bath immersion times.

As it was expected, the curves are shift towards the right of the figure when the bath immersion times increases. This indicates that the hardness of coatings is predominant into the hardness measurement of the coating/substrate couples, this results from the increase of the coating thickness versus the bath immersion time. Figure 4 shows that for the lower indenter depths resulting from the application of the lower indentation loads, the hardness obtained is rather constant and equal to 0·45 GPa approximately. This value corresponds to the hardness of the outer layer. When the indenter depths increase, the composite hardness increases and tends towards that of the substrate which has been found equal to 1·2 GPa independently on the applied load. Between these two limits, the analysis of indentation data has been carried out by considering that the external coating η is deformed plastically thus the value of $C^{(\eta)}$ is 0·1403, the second layer ξ as it is a soft film on a harder one then $C^{(\xi)}$ must be higher than 0·1403 and for the more internal coating layer δ which undergoes fracture, $C^{(\delta)}$ equals 0·0728. $C^{(\xi)}$ is found to be rather constant close to 0·4830. The values of hardness of each coating layer $H_F^{(i)}$ and the value of $C^{(\xi)}$ are assessed by a non-linear least square fitting. It is noticeable that the hardness is found to be independent on the bath immersion time, $H_F^{(\xi)} = 0.9$, $H_F^{(\xi)} = 0.9$ and $H_F^{(\delta)} = 3.1$ GPa. The value of $C^{(\xi)}$ is founded that is greater than 0·1403 for all the bath immersion times, which means that the normalised indentation depths must be greater than around 14% to influence to the composite hardness.

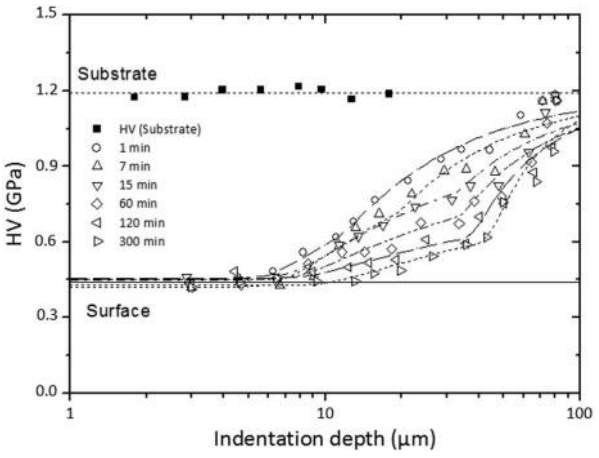

4 Hardness variation as a function of the indenter displacement into surface for the different bath immersion times.

To corroborate the predictive values of the hardness found for the different layers applying the multilayer model, the hardness-depth profile variation has been performed using the indentation load of 0·25 N in classical Vickers microindentation. Since the hardness-depth profiles are similar for the different bath immersion times, only the three specimen galvanised at immersion time of 15, 60 and 300 min have been shown. Figure 5*a* represents the Vickers hardness, $HV_{0·25}$, as a function of the distance from the interface between the coating and the substrate. Towards the substrate, it is considered the actual distance, x, whereas towards the coating we used the relative distance by considering the distance from the interface, x, to the total coating thickness, Y, ratio in order to highlight potential similarity between the different coatings according to the bath immersion times.

Figure 5*b* shows the indents which have been regularly performed along a cross-section of the coating obtained after 300 min of bath immersion. Owing to the low indentation load used, i.e. 0·25 N, the size of the indent diagonal is quite small. Indeed, their values are located between 13 and 30 µm which inevitably lead to a relative important standard deviation, around ±1 µm of the indent diagonal. Consequently, the two extreme values of the corresponding hardness are 2·8 ±0·5 GPa and 0·5±0·3 GPa, respectively, for 13 and 30 µm of the indent diagonal. Moreover, it can note in Fig. 5*a* that the indentation-depth profiles into the coating are not well-superimposed. This is due to the fact that the growth of the different layers depends on the bath immersion time. Additionally, the surface preparation of a cross-section can modified the mechanical behaviour of the coating. For example, we can assist to a relaxation of the residual stresses which affects the hardness measurement. Indeed, it is recognised that compressive residual stress hinders the indenter penetration, whereas the tensile test tends to facilitate its penetration.[22,23]

Independently on the bath immersion time, Fig. 5*a* reveals four distinct zones. In the first zone corresponding to the substrate, the hardness was found constant with a value of 1·15 GPa in accordance with the substrate hardness obtained when applying different indentation loads (Fig. 4). Close to the interface and into the

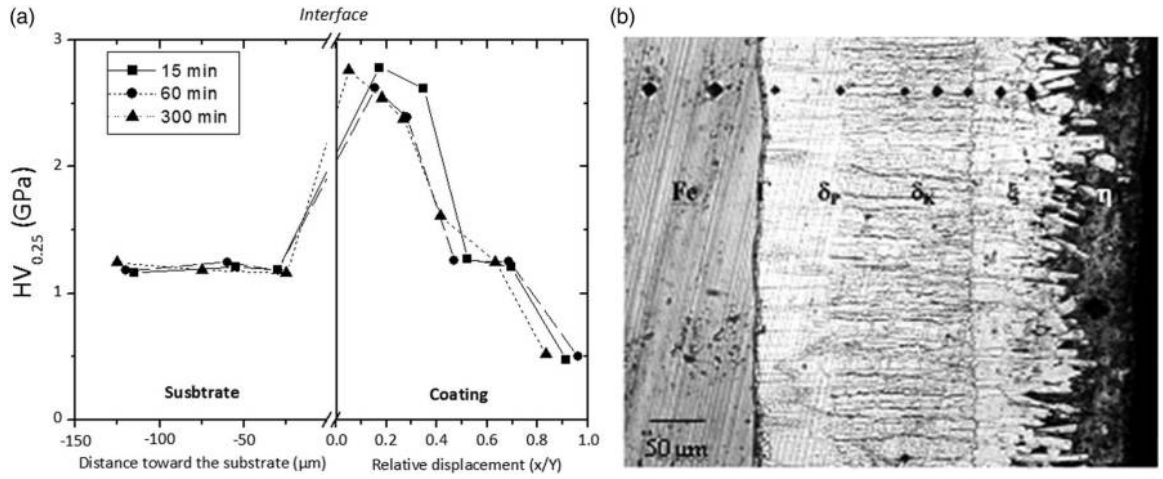

5 ***a*** **Hardness-depth profile obtained on the cross-sections of the coatings immersed during 15, 60 and 300 min and** ***b*** **microstructure and Vickers indent along a cross-section of the sample galvanised during 300 min.**

Table 3 Kinetic growth laws, constants $C^{(i)}$ and the hardness HV_F in GPa of each intermetallic compound layer

Intermetallic compounds	Kinetic growth law	$C^{(i)}$	HV_F (GPa)
δ-$FeZn_7$	$8.6 \times t^{0.50}$	0·0728	3·10
ξ-$FeZn_{13}$	$19.7 \times t^{0.25}$	0·4830	0·90
η-Zn	$32.8 \times t^{0.09}$	0·1403	0·45

coating, the hardness value of around 2·8 GPa is the maximum value obtained in the inner layer corresponding to the δ-$FeZn_7$ intermetallic compound. This value is in the same range of magnitude than the value of 3·1 GPa deduced from the application of the multilayer model. The intermediate zone related to the ξ-$FeZn_{13}$ intermetallic compound shows a hardness value slightly higher than 1·1 GPa and the hardness of the outer layer corresponding to the η-Zn phase is close to 0·5 GPa. These results agree well with the predictive values deduced from the application of the multilayer model developed by Rahmoun *et al.*[12] and with values available in literature collected in Table 1.

Hardness-load modelling

To predict the hardness variation as a function of the applied load, or in the same way as a function of the indenter displacement, the application of the model of Rahmoun *et al.*[12] extended by Puchi-Cabrera *et al.*[13] equations (4)–(7) requires the knowledge of the kinetic growth laws, the hardness and the corresponding constant C for each intermetallic compound layer. This was the objective of the first part of this study which allows to collect in Table 3 the parameters required for the application of the multilayer coating hardness model.

Consequently starting from the estimation of the coating thickness from the bath immersion time and the determination of the constant $C^{(i)}$ involved in the multilayered coating model, it is possible from now to express the different coefficients $a_F^{(i)}$ as a function of the indenter displacement where the adjusting parameter is the bath immersion time as it is shown in equations (8).

$$a_F{}^{(\eta)} = \begin{cases} 1 & \text{if } C^{(\eta)} \times 32.8t^{0.09} > h \\ 1 - \left(1 - \dfrac{C^{(\eta)} \times 32.8t^{0.09}}{h}\right)^2 & \text{otherwise} \end{cases}$$

$$a_F{}^{(\xi)} = \begin{cases} 1 - a_F{}^{(\eta)} & \text{if } C^{(\xi)} \times 19.7t^{0.25} > h \\ 1 - \left(1 - \dfrac{C^{(\xi)} \times 19.7t^{0.25}}{h}\right)^2 & \\ \quad - \left[1 - \left(1 - \dfrac{C^{(\eta)} \times 32.8t^{0.09}}{h}\right)^2\right] & \\ \text{otherwise} & \end{cases} \quad (8)$$

$$a_F{}^{(\delta)} = \begin{cases} 1 - \left(a_F{}^{(\eta)} + a_F{}^{(\xi)}\right) & \\ \quad \text{if } C^{(\delta)} \times 8.6t^{0.50} > h & \\ 1 - \left(1 - \dfrac{C^{(\delta)} \times 8.6t^{0.50}}{h}\right)^2 & \\ \quad - \left[1 - \left(1 - \dfrac{C^{(\xi)} \times 19.7t^{0.25}}{h}\right)^2\right] & \\ \text{otherwise} & \end{cases}$$

$$a_F{}^{(S)} = 1 - \left(a_F{}^{(\eta)} + a_F{}^{(\xi)} + a_F{}^{(\delta)}\right)$$

Where the constants $C^{(i)}$ are resumed in Table 3 as well as the kinetic growth laws which are implemented in the different expressions of the coefficients $a_F{}^{(i)}$.

Equation (8) can be now introduced in equation (7) to plot the hardness as a function of the indenter displacement for a given bath immersion time as follows:

$$H_C = a_F{}^{(S)} H_S + a_F{}^{(\eta)} H_F{}^{(\eta)} + a_F{}^{(\xi)} H_F{}^{(\xi)} + a_F{}^{(\delta)} H_F{}^{(\delta)} \quad (9)$$

Where the hardness of the different intermediate layers are collected in Table 3.

Figure 6 shows an example of application of equation (9) for bath immersion times of 1, 15 and 60 min which allows the comparison with the experimental indentation data. As

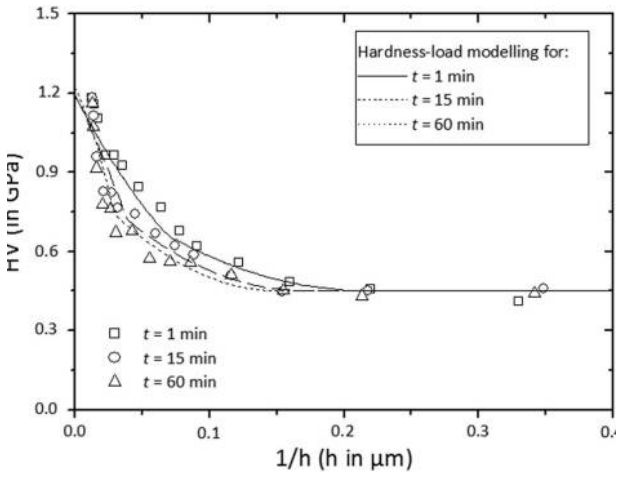

6 Prediction of the hardness-load variation applied to the bath immersion times of 1, 15 and 60 min and comparison with the experimental indentation data.

it is visible in Fig. 6, the model adequately represents the hardness variation as a function of the inverse of the indenter displacement, or dependently of the indentation load. Consequently, the model allows to estimate the hardness-load variation for a given bath immersion time and inversely to determine the deposition conditions for obtaining the required hardness-load variation.

Conclusions

The kinetic growth of the different layers follows a classical power law for which the coefficients depend on the nature of the layer. It was found that the delta phase (δ) growth is faster compared to the growths of zeta phase (ξ) and eta (η) phase. Moreover, the galvanisation coating presents heterogeneous layers δ, ξ and η-phase. For the higher bath immersion times, the gamma phase (Γ) is present as thin layer and the δ-phase layer occupies the most important proportion of the coating, whereas it is the η-phase for the lowest ones. A multilayer model allows to separate the contribution of the different layers of the coating and the determination of the hardness of the different intermetallic compounds independently on the bath immersion time. The predictive values of 3·1, 0·9 and 0·45 GPa were obtained for the δ-$FeZn_7$, ξ-$FeZn_{13}$ intermetallic compounds and the η-Zn phase, respectively. The methodology proposed predicts hardness-load variation from kinetic growth laws, hardness of the intermetallic compounds and multilayer coating model, and inversely it allows to determine deposition conditions to obtain a required hardness-load variation.

ORCID

D Chicot http://orcid.org/0000-0002-5203-3168

References

1. D. Horstmann: '*Reaction between iron and zinc*', 1978, London, Zinc Development Association.
2. A. R. Marder: 'The metallurgy of zinc-coated steel', *Prog. Mater. Sci.*, 2000, ***45***, 191–271.
3. P. Bicao, W. Jianhua, S. Xuping, L. Zhi and Y. Fucheng: 'Effects of zinc bath temperature on the coatings of hot-dip galvanizing', *Surf. Coat. Technol.*, 2008, ***202***, 1785–1788.
4. D. Horstmann and F. K. Peters: 'The reaction between iron and zinc', Proceeding of the 9th International Hot Dip Galvanization Conference, Zinc Development Association, London, 1971.
5. C. E. Jordon and A. R. Marder: 'Fe-Zn phase formation in interstitial-free steels hot-dip galvanized at 450°C: Part I 0.00 wt% Al-Zn baths', *J. Mater. Sci.*, 1997, ***32***, 5593–5602.
6. D. Horstmann: 'Formation and growth of iron-zinc alloy layers', Proceeding of the 14th International Hot Dip Galvanization Conference. Zinc Development Association, London, 1986, 1–6.
7. M. Onishi, Y. Wakamatsu and H. Miura: 'Formation and growth kinetics of intermediate phases in Fe-Zn diffusion couples', *Trans. JIM*, 1974, ***15***, 331–336.
8. G. F. Bastin, F. J. J. Van Loo and G. D. Rieck: 'A new compound in the iron zinc system', *Zeitschrift für Metallkunde*, 1977, ***68***, 359–361.
9. G. Vourlias, N. Pistofidis, G. Stergioudis and D. Tsipas: 'The effect of alloying elements on the Crystallization behaviour and on the properties of galvanized coatings', *Cryst. Res.*, 2004, ***39***, 23–29.
10. A. R. B. Verma and W. J. Van Ooij: 'High-temperature batch hot-dip galvanizing. Part 2. Comparison of coatings formed in the temperature range 520–555 °C', *Surf. Coat. Technol.*, 1997, ***89***, 143–150.
11. C. E. Jordon and A. K. Marder: 'Morphology development in hot-dip galvanneal coatings', *Metall. Mater. Trans. A.*, 1994, ***25***, (5), 937–947.
12. K. Rahmoun, A. Iost, V. Keryvin, G. Guillemot and N. E. Chabane Sari: 'A multilayer model for describing hardness variations of aged porous silicon low-dielectric-constant thin films', *Thin Solid Films*, 2009, ***518***, 213–221.
13. E. S. Puchi-Cabrera, M. H. Staia and A. Iost: 'Modeling the composite hardness of multilayer coated systems', *Thin Solid Films*, 2015, ***578***, 53–62.
14. B. Jönsson and S. Hogmark: 'Hardness measurements of thin films', *Thin Solid Films*, 1984, ***114***, 257–269.
15. H. Bückle: 'L'essai de microdureté et ses applications', vol. 90, Publications Scientifiques et Techniques du Ministère de l'Air, Paris, 1960.
16. H. Bückle: 'Use of the hardness test to determine other materials properties', in '*Science of Hardness Testing and Its Research Applications*', (edsJ. H. Westbrook and H. Conrad), Vol. ***453***, 1971, OH, ASM, Metals park.
17. A. Iost, D. Najjar and R. Hellouin: 'Modelling of the Vickers hardness of paint coatings deposited on metallic substrates', *Surf. Coat. Technol.*, 2003, ***165***, 126–132.
18. R. Saha and W. D. Nix: 'Effects of the substrate on the determination of thin film mechanical properties by nanoindentation', *Acta Mater.*, 2002, ***50***, 23–38.
19. X. Chen and J. J. Vlassak: 'Numerical study on the measurement of thin film mechanical properties by means of nanoindentation', *J. Mater. Res.*, 2001, ***16***, 2974–2982.
20. N. L. Okamoto, M. Inomoto, H. Adachi, H. Takebayashi and H. Inui: 'Micropillar compression deformation of single crystals of the intermetallic compound ζ-$FeZn_{13}$', *Acta Mater.*, 2014, ***65***, 229–239.
21. N. L. Okamoto, D. Kashioka, M. Inomoto, H. Inui, H. Takebayashiand and S. Yamaguchi: 'Compression deformability of Γ and ζ Fe–Zn intermetallics to mitigate detachment of brittle intermetallic coating of galvannealed steels', *Scripta Mater.*, 2013, ***69***, 307–310.
22. E. Frutos, M. Multigner and J. L. González-Carrasco: 'Novel approaches to determining residual stresses by ultramicroindentation techniques: application to sandblasted austenitic stainless steel', *Acta Mater.*, 2010, ***58***, 4191–4198.
23. C. E. Keutenedjian Mady, S. A. Rodriguez, A. G. Gómez and R. M. Souza: 'Numerical analysis of different methods to calculate residual stresses in thin films based on instrumented indentation', *J. Mater. Res.*, 2012, ***27***, 1732–1741.